Quantum band engineering of nitride semiconductors for infrared lasers

O. Malis,[a,*] C. Edmunds,[a] D. Li,[a,b] J. Shao,[a,b] G. Gardner,[b,c] W. Li,[d] P. Fay,[d] and M. J. Manfra,[a,b,c,e]
[a]Department of Physics, Purdue University, West Lafayette, Indiana 47907, USA;
[b]Birck Nanotechnology Center, West Lafayette, Indiana 47907, USA;
[c]School of Materials Engineering, Purdue University, West Lafayette, Indiana 47907, USA;
[d]Dept. of Electrical Engineering, University of Notre Dame, Notre Dame, IN 46556, USA;
[e]School of Electrical and Computer Engineering, Purdue University, West Lafayette, Indiana 47907, USA;
*Author e-mail address: omalis@purdue.edu

ABSTRACT

The III-nitride semiconductors have been proposed as candidate materials for new quantum cascade lasers in the near-infrared (1.5-3 μm), and far-infrared (30-60 μm), due to the large conduction-band offset between GaN and Al-containing alloys (>1 eV), and the large longitudinal optical (LO) phonon energy (90 meV), respectively. The challenges of III-nitride intersubband devices are twofold: material and design related. Due to large electron effective mass, the nitride intersubband materials require the ability to fine-tune the atomic structure at an unprecedented sub-nanometer level. Moreover, the III-N materials exhibit built-in polarization fields that complicate the design of intersubband lasers. This paper presents recent results on c-plane nitride resonant-tunneling diodes that are important for the prospects of far-infrared nitride lasers. We also report near-infrared absorption and photocurrent measurements in nonpolar (m-plane) AlGaN/GaN superlattices.

Keywords: intersubband transitions, quantum cascade lasers, nitride semiconductors

1. INTRODUCTION

The III-nitride heterostructures have unique electronic and optical properties that make them promising for extending the functionality of semiconductor optoelectronics into spectral ranges currently inaccessible with other material systems. The III-nitride system has been proposed as a candidate for new lasers and detectors in the near-infrared (1.5-3 μm), and far-infrared or Terahertz (30-60 μm) range, due to the large conduction-band offset between GaN and Al-containing alloys (>1 eV), and the large longitudinal optical (LO) phonon energy (90 meV), respectively.[1,2] These devices employ intersubband transitions in the conduction band and operate using the general principles of quantum cascade lasers (QCLs) and quantum well infrared photodetectors (QWIPs). The challenges of nitride intersubband devices are two-fold: material-related and design-related.[2] The material issues are given by the impact of defects and nanostructure on the electronic band structure. With the continuous improvement of GaN substrate technology and epitaxial growth, the material-related issues have been tremendously reduced over the past years. Remaining materials challenges are related to the impact of the nanostructure on infrared optical properties. Due to large electron effective mass, the nitride intersubband materials require the ability to fine-tune the atomic structure at an unprecedented sub-nanometer level. We have performed in-depth studies of the impact of nanostructure and doping on near-infrared absorption in AlGaN/GaN and AlInN/GaN heterostructures for near-infrared intersubband devices.[3-6] We also observed for the first time exactly reproducible low-temperature negative differential resistance in c-plane resonant tunneling diodes on low-defect quasi-bulk GaN substrates.[7,8] This paper focuses on recent data on c-plane resonant tunneling diodes. These results are important for the prospects of THz QCLs.

The design issues of nitride QCLs are to a large extent due to the presence of built-in polarization fields in nitride heterostructures on c-plane GaN. An important and virtually unexplored path to reducing the influence of polarization fields in infrared optoelectronic devices is the use of heterostructures on non-polar orientations (such as the m-plane or

Novel In-Plane Semiconductor Lasers XIII, edited by Alexey A. Belyanin,
Peter M. Smowton, Proc. of SPIE Vol. 9002, 90021D · © 2014 SPIE
CCC code: 0277-786X/14/$18 · doi: 10.1117/12.2036286

a-plane) of GaN. For nonpolar oriented GaN, the polarization vector lies in the plane perpendicular to the growth direction and thus there are no polarization discontinuities at heterojunctions. In addition to simplification of device modeling under flat band conditions, some immediate advantages of structures on nonpolar GaN include improved optical dipole matrix elements and increased confinement for high lying energy levels. We report near-infrared intersubband absorption and photocurrent measurements in m-plane AlGaN/GaN superlattices. These results open the path for future infrared m-plane nitride devices.

2. THEORETICAL MODELING OF NITRIDE QCLS

Design of nitride QCLs presents some unique challenges related to the intrinsic properties of the materials, such as built-in polarization fields, and large effective masses. These properties are particularly restricting for near-infrared QCLs. Moreover, even though several theoretical structures have been proposed for near-infrared lasers using Al(Ga)N/GaN heterostructures, practical realization of these devices has been hampered by the large lattice-mismatch between AlN and GaN.[1] An important, yet sometimes overseen requirement of QCLs is that they consist of a large number of quantum wells (QWs) and barriers (> 500) adding up to epilayer thicknesses beyond the critical thickness corresponding to any significant Al-composition alloy. The lasers, in particular, need to be considerably thicker epilayers than the visible/UV devices (>2 μm thick) due to the need to provide optical confinement in the infrared, and therefore cannot tolerate any amount of strain. To date, near-infrared emission in nitrides has been observed only in relatively-thin optically-pumped multiple QWs.[1]

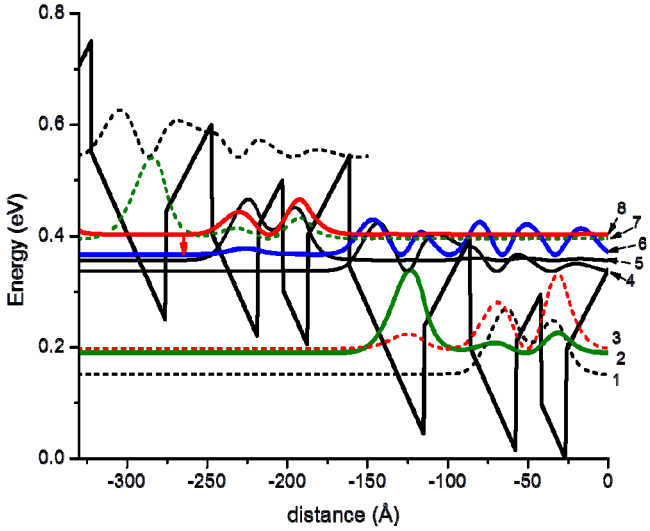

Figure 1. Conduction band diagram and the most significant wave functions for 2-repeats of a nitride THz QCL active region designed for operation at 30-μm. The laser transition is indicated by the red arrow.

The lattice-mismatch challenge is somewhat alleviated for far-infrared devices because they employ relatively low Al content AlGaN barriers. For example, the THz nitride QCL proposed theoretically by Sun et al.[9] uses GaN for the well material and $Al_{0.15}Ga_{0.85}N$ for the barriers. For this reason, more progress towards THz emitters has been achieved than towards near-infrared emitters. THz electroluminescence has been reported in structures that exploit the longitudinal optical (LO) phonon extraction mechanism that has been successful in GaAs THz QCLs.[10,11]

Due to the lattice-mismatch challenge we have been focusing on exact lattice-matched AlInGaN/GaN heterostructures that are promising for both near- and far-infrared laser applications. Moreover, the polarization fields in lattice-matched AlInGaN/GaN heterostructures are significantly reduced compared to GaN/AlGaN due to lack of piezoelectric polarization. Fig. 1 shows the band diagram and most relevant electron wave functions for a THz lattice-matched nitride QCL we propose for operation at 30-μm. The structure takes advantage of the most successful design concepts from GaAs THz QCLs. The active unit consists of 3 GaN quantum wells separated by $Al_{0.164}Ga_{0.8}In_{0.036}N$ barriers. The CBO for this material combination was approximated to be 0.2 eV, and the intrinsic polarization to be 0.6 MV/cm. Electrons are injected through tunneling into level 8, undergo an optical transition from levels 8 to 6, and then are extracted

through tunneling to level 4 and LO-phonon scattering to levels 3 and 2. The optical gain coefficient, g, for a 3-level QCL is given by:[12]

$$g = \tau_3\left(1-\frac{\tau_2}{\tau_{32}}\right)\frac{4\pi e z_{32}^2}{\lambda\varepsilon_0 n_{ef} L_p}\frac{1}{2\gamma_{32}}$$

where τ_3 is total upper-state lifetime, τ_2 is the total lifetime of level 2 (lower laser level) and τ_{32} is the lifetime for the 3-2 transition. z_{32} is the dipole moment matrix element for the laser 3-2 transition, n_{ef} the effective refractive index at wavelength λ, L_p the thickness of one active region and injector, ε_0 the vacuum dielectric constant, e the elementary charge, and $2\gamma_{32}$ the full width at half maximum of the luminescence spectrum. This expression highlights the parameters that are essential for intersubband laser operation: the lifetimes, optical dipole matrix element, and optical transition width.

For the structure in Fig. 1, the optical matrix dipole moment z_{86} was calculated to be 1.5-nm. Unlike the case of GaAs THz QCLs, for nitride THz QCLs the upper laser lifetime (τ_3) is dominated by LO phonon scattering and was estimated based on the Fröhlich interaction to be 2.2 ps. In spite of the picosecond laser lifetime (similar to mid-infrared QCLs), τ_{32} will always be longer than τ_2 and therefore population inversion can be maintained. Assuming that τ_2 = 60 fs $<<\tau_{32}$, we neglected the term in the parentheses in the gain formula, and estimated the optical gain for the structure in Fig. 1 to be 79 cm/kA. This value is promising for achieving room-temperature lasing in double metal waveguides, and is also in agreement with other calculations for nitride QCL structures.

The design challenges of nitride intersubband devices are to a large extent related to the presence of polarization fields in nitride heterostructures on c-plane GaN. An important and little explored path to reducing the influence of built-in polarization fields in infrared optoelectronic devices is the use of heterostructures on non-polar orientations (such as the m-plane) of GaN. For m-plane oriented GaN, the polarization vector lies in the plane perpendicular to the growth direction and thus there are no polarization discontinuities at heterojunctions. The effect of the polarization fields on the band structure is illustrated in Fig. 2(a) as compared to Fig. 2(b). In addition to simplification of device modeling under flat band conditions, some immediate advantages of structures on nonpolar GaN include improved optical dipole matrix elements and increased confinement for high lying energy levels. Fig. 2(c) shows the expected enhancement of intersubband absorption for m-plane as opposed to c-plane QWs.

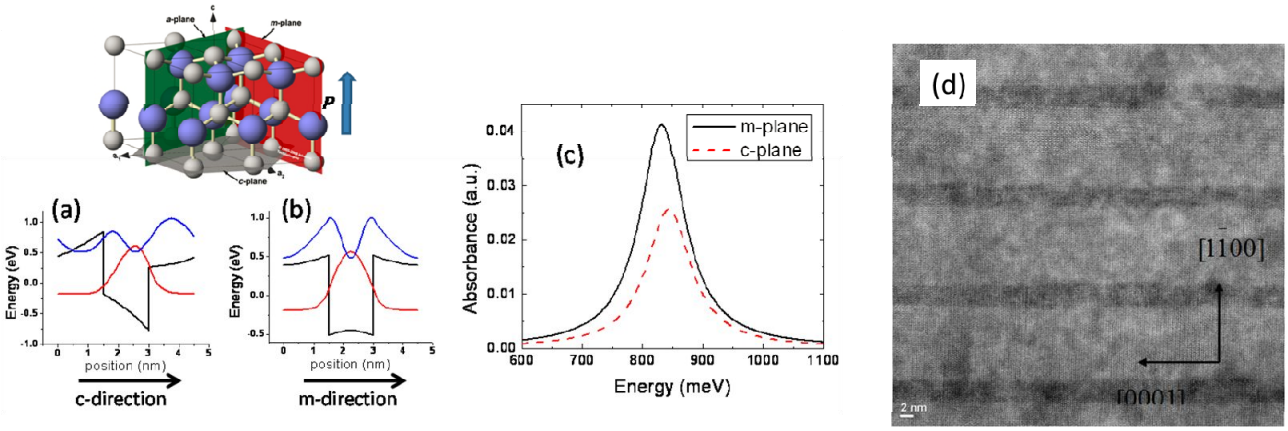

Figure 2. Comparison of the conduction band diagram on c-plane (a) and m-plane (b) for a 1.5-nm GaN QW with 2.8-nm $Al_{0.55}Ga_{0.45}N$ barriers. (c) Comparison of theoretical near-infrared absorption spectra for the QW on c- and m-plane GaN. (d) HR-TEM image of an m-plane AlGaN/GaN superlattice.

The absence on built-in polarization fields in m-plane nitride heterostructures facilitates the design of near-infrared nitride QCLs and reduces the Al concentration needed in the AlGaN barriers. Fig. 3 shows the band diagram and most relevant electron wave functions for a near-infrared nonpolar nitride QCL we propose for operation at 2.8-μm. The active unit consists of 9 GaN QWs separated by $Al_{0.55}Ga_{0.45}N$ barriers (CBO≈1 eV). Electrons are injected through tunneling into level 3, undergo an optical transition from levels 3 to 2, and then are extracted through LO-phonon

scattering to level 1. For the structure in Fig. 3, z_{32} was calculated to be 0.23-nm. τ_3 is dominated by LO phonon scattering and was estimated to be 1.2 ps. We estimated the optical gain for the structure in Fig. 3 to be 2.3 cm/kA, value that is promising for achieving lasing in devices with dielectric waveguides.

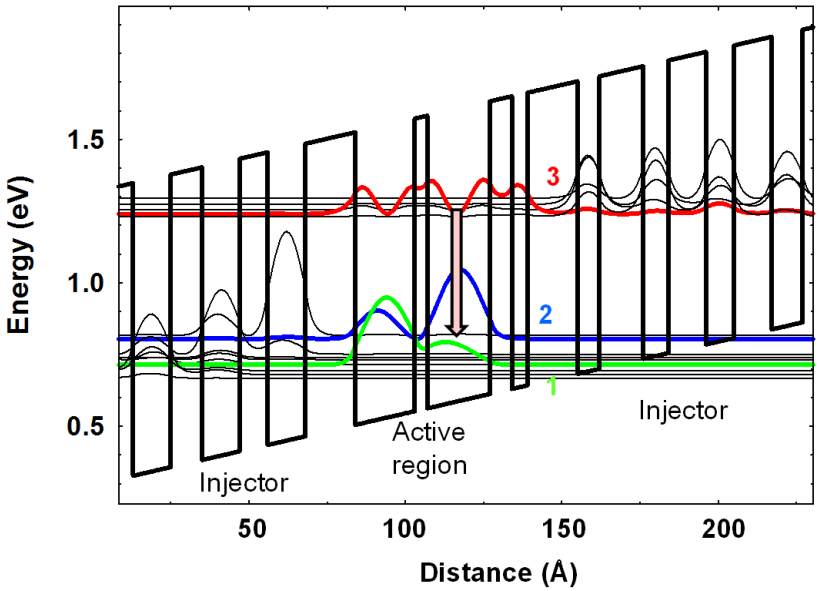

Figure 3. Conduction band diagram and the most significant wave-functions of the active region/injector of an m-plane nitride QCL designed for operation at 2.8-μm. The laser transition is indicated by the block arrow.

Besides the gain medium, the optical cavity is the second major component of a laser that drastically affects its operation. To achieve laser action the gain has to exceed the waveguide and mirror losses. The threshold current density is given by: $J_{th}=(\alpha_w+\alpha_m)/g\Gamma$, where α_w and α_m are the waveguide and mirror losses, g is the gain coefficient and Γ is the optical mode confinement factor. Waveguide losses in QCLs are calculated by solving the wave equation for the waveguide taking into account material losses. Material losses in the infrared are dominated by free carrier absorption and can be estimated using the Drude model. Our preliminary investigations into the waveguide structure for a 2.8-μm nonpolar nitride QCL suggest that light confinement can be effectively obtained by varying the doping density in GaN layers (plasmon-enhanced layers). A threshold current density of ~12 kA/cm^2 was estimated at low temperature, value that is well within experimental measurement capabilities.

3. EXPERIMENTS

The progress towards nitride infrared lasers has been slowed down to a larger extent than their visible counterparts by the scarcity of high-quality native substrates. In the early studies, the material issues were dominated by the high density of defects present in structures grown on non-native substrates. The materials for the first studies of intersubband absorption were grown on sapphire and therefore had a large number of threading dislocations (>10^{10} cm^{-2}) due to the large lattice mismatch between GaN and sapphire. While providing promising optical results, these materials were not sufficient for vertical transport devices. Driven mainly by the need for higher-quality GaN substrates for visible lasers, the nitride substrate technology has evolved tremendously though over the past 10 years. The single-crystal substrates are still small and prohibitively expensive, but high-quality free-standing GaN substrates (dislocation density ~10^6 cm^{-2}) and templates grown by hydride vapor-phase epitaxy (HVPE) are now commercially available. Our nitride intersubband structures are grown by plasma-assisted molecular beam epitaxy (MBE) on free-standing GaN substrates from Kyma Technologies. After growth, the structural properties of the materials are characterized with atomic force microscopy (AFM), high-resolution transmission electron microscopy (HR-TEM), and high-resolution x-ray diffraction (HR-XRD).[2]

With the advances in production of low-defect density nitride substrates, other more subtle material limitations such as layer interdiffusion, interface roughness, alloy inhomogeneity, etc. have come into focus.[3,4] Due to the high electron effective mass, the nitride QWs and barriers need to be extremely thin. As a result, the confined states in the conduction band are extremely sensitive to structural properties such as layer thickness and composition uniformity, interface

roughness, etc. Moreover, the high doping levels needed to observe near-infrared absorption has indirect effects on structural quality and intersubband transition linewidth.[4] Therefore, it is fair to state that the material requirements for intersubband devices are considerably more stringent than for visible/UV optoelectronics.

While the potential theoretical advantages of a non-polar QCL design are clear, the material growth modes and microstructure of non-polar heterostructures have not been studied in as much detail as those of the polar (c-plane) structures. It is noteworthy that recent substrate developments resulted in growth of thick boules of c-plane GaN from which non-polar oriented substrates (a- and m-plane) can be harvested [28]. These bulk substrates appear to be the ideal platform to investigate non-polar III-nitride heterostructures for infrared lasers. We have succeeded in growing m-plane GaN and AlGaN/GaN superlattices by MBE on free-standing $(1\bar{1}00)$ GaN substrates from Kyma Technologies and performed several detailed studies of their microstructure.[13,14] Two-dimensional and homogeneous growth of AlGaN was achieved through careful control of the III/V flux ratio. AlN island nucleation often reported for m-plane AlGaN under nitrogen-rich growth conditions was suppressed using high III/V flux ratios. Fig. 2(d) shows the HR-TEM image of an m-plane AlGaN/GaN superlattice designed for far-infrared absorption measurements.

The optical properties of polar and nonpolar nitride superlattices were characterized with infrared spectroscopy. The direct infrared intersubband absorption of strained AlGaN/GaN superlattices on c- and m-plane GaN Kyma substrates was measured using a Thermo-Nicolet Fourier-transform infrared (FT-IR) spectrometer, a wire-grid polarizer, and a beam condenser. In the case of m-plane AlGaN/GaN superlattices, the absorption was too small to measure in single-pass geometry. Therefore, the facets of the sample were polished at 45° in order to fabricate multi-pass waveguides. The optical spectra were obtained for both p- and s-polarizations using the internal white light source of the spectrometer and a liquid nitrogen cooled InSb detector. The p- and s-polarized spectra were normalized to reference spectra taken in the absence of any sample. Photo-induced absorption measurements were also performed using an optically chopped 15 mW HeCd laser operating at 325 nm to modulate the electron density while the differential transmission was measured in step-scan mode with a lock-in amplifier.

Large infrared photodetector and small-area resonant-tunneling devices were processed using procedures developed from reports in the literature. Standard photolithography was used to pattern resist for mesa definition. Depending on the type of the devices the mesas varied from 4×4 μm^2 (resonant tunneling diodes) to 500×2000 μm^2 (infrared photodetectors). Nitride semiconductor patterning was done using chlorine based ICP-RIE dry etching. In this step, we have optimized the etching parameters such as reactive gas flow rate, plasma power, forward bias, etc., to get smooth sidewalls and optimal etching rate. Several techniques are employed to reduce the plasma-induced defects, such as nitrogen plasma surface passivation, high temperature rapid thermal annealing (RTA) and wet chemical etching. The dry etching is followed by PECVD growth of 300nm SiO_2 at 300°C for electrical insulation and surface passivation. A second photolithography step is conducted on the SiO_2 covered mesa in order to open windows for top and bottom contacts. This photolithography step is the most challenging processing step for the fabrication of resonant tunneling diodes because it requires alignment with a precision better than 1 μm. Lithography is followed by ICP-RIE etching of the SiO_2. A third photolithography and metallization step is used for deposition of the contact materials. The metal stack consisting of Ti/Al/Ni/Au is deposited by e-beam evaporation at room temperature and patterned via lift-off. Finally, the samples are rapidly thermally annealed in a nitrogen atmosphere at 530°C to achieve ohmic contacts for the top and bottom contact layers. The optimal annealing temperature and time were established with transmission-line measurements of the contact resistivity. The semiconductor chips were mounted on Cu heat sinks and wire-bonded to Au pads. The temperature-dependent current-voltage (I-V) characteristics or photocurrent response for resonant tunneling diodes and photodetectors, respectively, were measured in a liquid nitrogen-flow cryostat.

4. EXPERIMENTAL RESULTS

To evaluate the feasibility of nitride QCLs, we have studied vertical transport in intersubband nitride heterostructures. The double-barrier resonant tunneling diode (RTD) is the simplest device to explore quantum vertical transport. RTDs show negative differential resistance (NDR) in the current-voltage (I-V) characteristics associated with resonant tunneling through quantized states in a single quantum well. This well-known phenomenon has been extensively investigated in arsenide heterostructures. In all arsenide devices, it was found that the peak-to-valley ratio (PVR) increases with decreasing temperature, and that the I-V characteristics are exactly reproducible for the same device upon repeated measurement. In contrast, resonant tunneling in nitride thin film devices has been challenging to prove. Research on electron vertical transport in GaN/Al(Ga)N RTDs at room-temperature has been reported by several groups.[1] Most papers, though, show that the NDR in c-plane RTDs appears only during the forward bias sweep of the I-

V characteristics. In some cases the NDR disappears during backward voltage sweep while in others it disappears for subsequent forward voltage scans. It is noteworthy that NDR in nitrides has also been observed experimentally in nonpolar AlN/GaN double-barrier RTDs and in defect-free nanowires.[1]

By taking advantage of progress in GaN substrate technologies and optimizing the MBE growth process to improve surface/interface roughness, we recently were able to report exactly-repeatable NDR signatures at 77 K in small-area c-plane $Al_{0.2}Ga_{0.8}N$/GaN RTDs grown on free-standing GaN substrates.[7,8] To identify the origin of NDR signatures in nitride RTDs, we carefully examined the temperature dependence of the I-V characteristics.[8] Fig. 4(b) shows the temperature dependence of the I-V characteristics of a nitride RTD consisting of a 2.4 nm GaN quantum well with $Al_{0.35}Ga_{0.65}N$ barriers. The negative NDR signature of resonant tunneling transport emerges below 140 K. This suggests that tunneling at high temperature is obscured by charge trapping. The maximum PVR we observed to date is 1.4 at 77 K in an RTD with a 4.9 nm well and $Al_{0.2}Ga_{0.8}N$ barriers (Fig. 4(c)). Interestingly, this device shows NDR even at room temperature in pulsed mode as shown in Fig. 4(d). We believe the performance of c-plane nitride RTDs is still limited by parallel conduction likely through dislocations, and by other defects that act as charge trapping sites. Since we did not succeed in measuring NDR in devices with Al concentration higher that 35% in the barriers, we can only speculate that the concentration of trapping sites is related to the Al-content in the barriers.

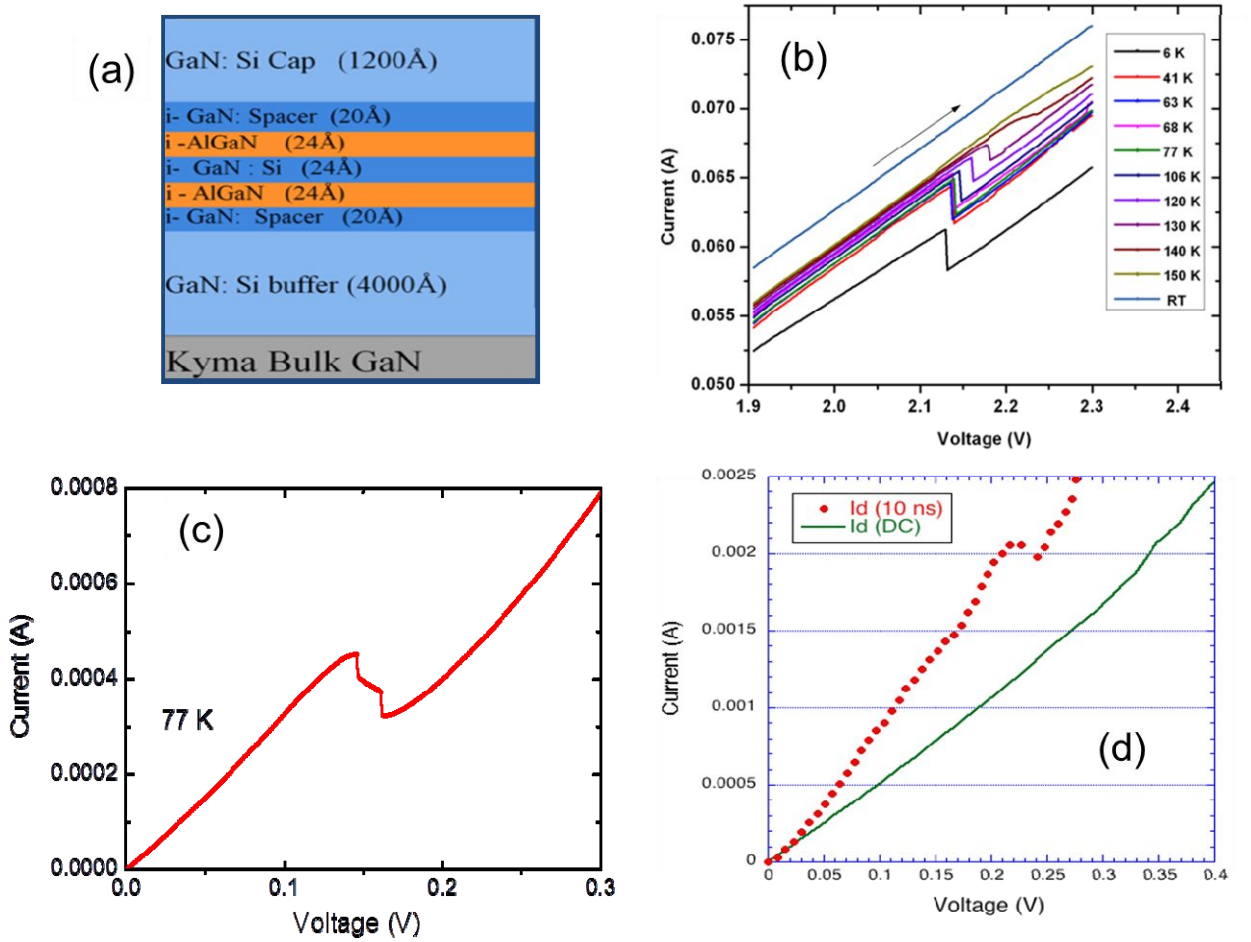

Figure 4. (a) Schematic of the layer structure of GaN/AlGaN RTDs. (b) Temperature-dependent I-V characteristics of a GaN/$Al_{0.35}Ga_{0.65}N$ RTD with a 2.4 nm quantum well measured from 6 K to room temperature. (c) I-V characteristics at 77 K of a GaN/$Al_{0.2}Ga_{0.8}N$ RTD with a 4.9 nm quantum well. (d) Room-temperature I-V characteristics measured in continuous more and in pulsed mode with 10 ns pulses of a GaN/$Al_{0.2}Ga_{0.8}N$ RTD with 4.9 nm quantum wells (same structure as the device characterized in (c)).

While considerable work has been done to study infrared absorption and infrared photodetectors using c-plane nitride heterostructures,[1] due to material growth difficulties relatively little data is available for nonpolar nitride materials.[15] We employed near-infrared absorption spectroscopy to characterize the infrared optical properties of nonpolar nitride heterostructures, to identify the nitride material parameters relevant to intersubband transitions, and to examine the effect of the growth conditions on the energy and linewidth of the intersubband absorption. We were able to observe, for the first time, near-infrared absorption at 1.75 μm in an m-plane $Al_{0.55}Ga_{0.45}N$/GaN superlattice (Fig. 5(a)). The energy of the transition is consistent with calculations performed with the nextnano3 simulation package. Moreover, infrared photodetectors were fabricated from m-plane $Al_{0.55}Ga_{0.45}N$/GaN superlattices and their photocurrent response was measured from room-temperature to 4 K. Fig. 5(b) shows the p- and s-polarized photocurrent at 5 K. The p-polarized signal is considerably stronger than the s-polarized signal indicating the intersubband origin of the optical transition. It is noteworthy that the polarization sensitive spectra are visible only at low temperature.

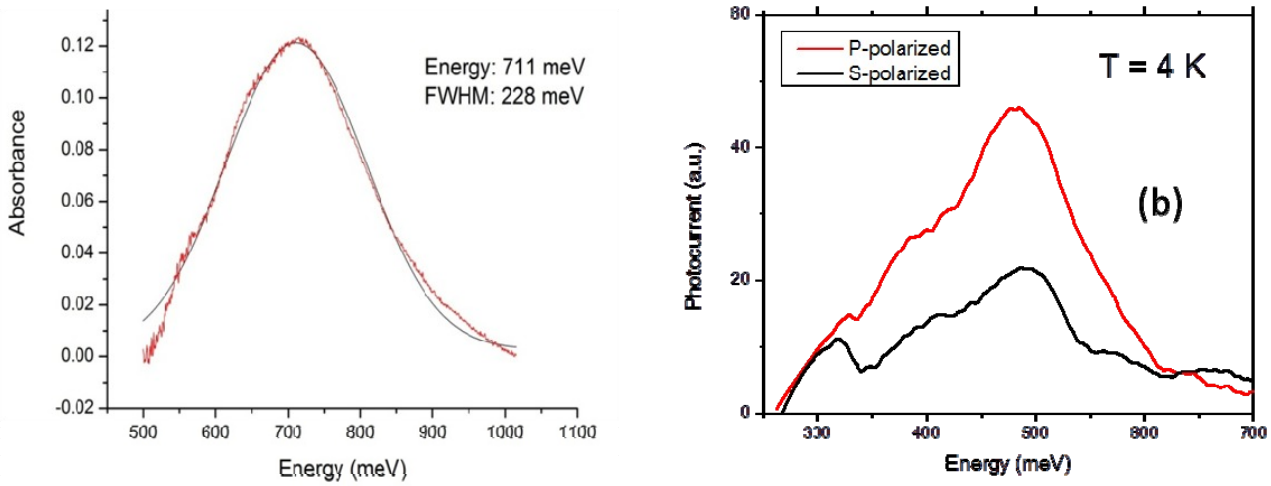

Figure 5. (a) Room-temperature near-infrared absorption from an m-plane $Al_{0.55}Ga_{0.45}N$/GaN superlattice. (b) P- and S-polarized photocurrent measured at 4 K from an m-plane $Al_{0.55}Ga_{0.45}N$/GaN superlattice.

5. CONCLUSIONS

In conclusion, the intersubband transitions in III-nitride multi-quantum well structures are been studied for their applications in novel infrared lasers. Progress of active devices such as the nitride quantum cascade lasers has been slowed down considerably by issues related to material defects and design challenges due to the built-in polarization fields in heterostructures on c-plane GaN. While tremendous progress has been made the last few years to reduce substrate defect densities, and further progress is expected to occur in the immediate future, our results on c-plane nitride RTDs indicate that the realization of the full potential of nitride infrared lasers is still limited by the properties of the available nitride substrates (defect density), the microstructure of the epitaxially grown heterostructures (interface roughness and interdiffusion, alloy non-uniformity, etc.), and the density of other defects acting as charge trapping sites.

In order to overcome the design challenges related to built-in fields, a potentially fruitful and relatively little explored direction of research is the use of non-polar substrates for intersubband devices. We were able to develop MBE growth conditions for m-plane AlGaN/GaN superlattices and to report for the first time near-infrared intersubband absorption and low-temperature photocurrent measurements in these structures.

ACKNOWLEDGEMENTS

This work was supported by the NSF awards ECCS-1001431, ECCS-1253720, and DMR-1206919; and the Defense Advanced Research Project Agency (DARPA) under contract no. D11PC20027. W. L. and P. F. acknowledge support from Dr. P. Maki at ONR.

REFERENCES

[1] Beeler, M., Trichas, E., and Monroy, E., "III-nitride semiconductors for intersubband optoelectronics: a review", Semicond. Sci. Technol. 28, 074022 (2013).

[2] Malis, O., "Nitride semiconductor materials for novel infrared optoelectronics", in New Developments in Photon and Materials Research, Ed. J. I. Jang, Nova Science Publishers, New York, p. 243 (2013).

[3] Edmunds, C., Tang, L., Shao, J., Grier, A., Li, D., Gardner, G., Zakharov, D. N., Ikonić, Z., Harrison, P., Manfra, M. J., and Malis, O., "Comparative study of near-infrared intersubband absorption in AlGaN/GaN and AlInN/GaN superlattices", Phys. Rev. B 88, 235306 (2013).

[4] Edmunds, C., Tang, L., Shao, J., Li, D., Cervantes, M., Gardner, G., Zakharov, D. N., Manfra, M. J., and Malis, O., "Improvement of near-infrared absorption linewidth in AlGaN/GaN superlattices by optimization of delta-doping location", Appl. Phys. Lett. 101, 102104 (2012).

[5] Edmunds, C., Tang, L., Li, D., Cervantes, M., Gardner, G., Paskova, T., Manfra, M. J., and Malis, O., "Near-infrared absorption in lattice-matched AlInN/GaN and strained AlGaN/GaN heterostructures grown by MBE on low-defect GaN substrates", J. Electron. Mat. 41, 881 (2012).

[6] Malis, O., Edmunds, C., Manfra, M. J., and Sivco, D. L., "Near-infrared intersubband absorption in molecular-beam epitaxy grown lattice-matched InAlN/GaN superlattices", Appl. Phys. Lett. 94, 161111 (2009).

[7] Li, D., Tang, L., Edmunds, C., Shao, J., Gardner, G., Manfra, M. J., and Malis, O., "Repeatable low-temperature negative-differential resistance from $Al_{0.18}Ga_{0.82}N$/GaN resonant tunneling diodes grown by molecular-beam epitaxy on free-standing GaN substrates", Appl. Phys. Lett. 100, 252105 (2012).

[8] Li, D., Shao, J., Tang, L., Edmunds, C., Gardner, G., Manfra, M. J., Malis, O., "Temperature-dependence of negative differential resistance in GaN/AlGaN resonant tunneling structures", Semicon. Sci. Technol. 28, 074024 (2013).

[9] Sun, G., Soref, R. A., and Khurgin, J. B., "Active region design of a terahertz GaN/$Al_{0.15}Ga_{0.85}N$ quantum cascade laser", Superlatt. Microstruct. 37, 107-113 (2005).

[10] Sudradjat, F., Zhang, W., Driscoll, K., Liao, Y. T., Bhattacharyya, A., Thomidis, C., Zhou, L., Smith, D. J., Moustakas, T. D., and Paiella, R., "Sequential tunneling transport characteristics of GaN/AlGaN coupled-quantum-well structures", J. Appl. Phys. 108, 103704 (2010).

[11] Terashima, W., and Hirayama, H., "Spontaneous emission from GaN/AlGaN terahertz quantum cascade laser grown on GaN substrate", Phys. Stat. Sol. C **8,** 2302 (2011).

[12] Gmachl, C., Capasso, F., Sivco, D. L., and Cho, A. Y., "Recent progress in quantum cascade lasers and applications", Rep. Prog. Phys. 64, 1533 (2001).

[13] Shao, J., Tang, L., Edmunds, C., Gardner, G., Malis, O., and Manfra, M. J., "Surface morphology evolution of m-plane ($1\bar{1}00$) GaN during MBE growth: impact of Ga/N ratio, miscut direction, and growth temperature", J. Appl. Phys. 114, 023508 (2013).

[14] Shao, J., Tang, L., Edmunds, C., Zakharov, D. N., Malis, O., and Manfra, M. J., "Strain relaxation in AlGaN/GaN superlattices grown on free-standing m-plane (1-100) GaN substrates", Appl. Phys. Lett. 103, 232103 (2013).

[15] Pesach, A., Gross, E., Huang, C.-Y., Lin, Y.-D., Vardi, A., Schacham, S. E., Nakamura, S., and Bahir, G., "Nonpolar m-plane intersubband based InGaN/(Al)GaN quantum well infrared photodetectors", Appl. Phys. Lett. 103, 022110 (2013).